

University of Groningen

Unraveling the Thermal Isomerization Mechanisms of Heteroaryl Azoswitches

Crespi, Stefano; Simeth, Nadja A.; Bellisario, Alfredo; Fagnoni, Maurizio; Koenig, Burkhard

Published in:
Journal of Physical Chemistry A

DOI:
[10.1021/acs.jpca.8b11734](https://doi.org/10.1021/acs.jpca.8b11734)

IMPORTANT NOTE: You are advised to consult the publisher's version (publisher's PDF) if you wish to cite from it. Please check the document version below.

Document Version
Publisher's PDF, also known as Version of record

Publication date:
2019

[Link to publication in University of Groningen/UMCG research database](#)

Citation for published version (APA):

Crespi, S., Simeth, N. A., Bellisario, A., Fagnoni, M., & Koenig, B. (2019). Unraveling the Thermal Isomerization Mechanisms of Heteroaryl Azoswitches: Phenylazoindoles as Case Study. *Journal of Physical Chemistry A*, 123(9), 1814-1823. <https://doi.org/10.1021/acs.jpca.8b11734>

Copyright

Other than for strictly personal use, it is not permitted to download or to forward/distribute the text or part of it without the consent of the author(s) and/or copyright holder(s), unless the work is under an open content license (like Creative Commons).

The publication may also be distributed here under the terms of Article 25fa of the Dutch Copyright Act, indicated by the "Taverne" license. More information can be found on the University of Groningen website: <https://www.rug.nl/library/open-access/self-archiving-pure/taverne-amendment>.

Take-down policy

If you believe that this document breaches copyright please contact us providing details, and we will remove access to the work immediately and investigate your claim.

Downloaded from the University of Groningen/UMCG research database (Pure): <http://www.rug.nl/research/portal>. For technical reasons the number of authors shown on this cover page is limited to 10 maximum.

Unraveling the Thermal Isomerization Mechanisms of Heteroaryl Azoswitches: Phenylazoindoles as Case Study

Stefano Crespi,[†] Nadja A. Simeth,[‡] Alfredo Bellisario,[§] Maurizio Fagnoni,^{*,||} and Burkhard König^{*,†} [†]Institut für Organische Chemie, Universität Regensburg, Universitätsstrasse 31, 93040 Regensburg, Germany[‡]Stratingh Institute for Chemistry, University of Groningen, Nijenborgh 7, 9747 AG Groningen, The Netherlands[§]Department of Physics, University of Pavia, Via Bassi 6, 27100 Pavia, Italy^{||}PhotoGreen Lab, Department of Chemistry, University of Pavia, Via Taramelli 12, 27100 Pavia, Italy

Supporting Information

ABSTRACT: The research on heteroaromatic azoswitches has been blossoming in recent years due to their astonishingly broad range of properties. Minimal chemical modifications can drastically change the demeanor of these switches, regarding photophysical and (photo)chemical properties, promoting them as ideal scaffolds for a vast variety of applications based on bistable light-addressable systems. However, most of the characteristics exhibited by heteroaryl azoswitches were found empirically, and only a few works focus on their rationalization. Herein we report on a mechanistic study employing phenylazoindoles as a model reference, combining spectroscopic experiments with comprehensive computational analysis. This approach will elucidate the intrinsic correlations between the molecular structure of the switch and its thermal behavior, allowing a more rational design transferable to various heteroaryl azoswitches.



INTRODUCTION

Arylazo compounds have undisputedly become one of the fundamental photoswitchable cores studied in the last decades.^{1,2} The molecular-scale motion of these compounds can be triggered by irradiation with light of a suitable wavelength, eventually forming the metastable *Z*-form.³ The reverse reaction restoring the stable *E*-starting material can be triggered by either photochemical or thermal means (Chart 1A).^{1,4–8} The thermal isomerization to the *E*-form is classically described following three different mechanisms and associated with characteristic lifetimes (τ) of the *Z*-isomer spanning from nanoseconds and several months (Chart 1B). The inversion mechanism can be simplified by an in-plane motion of a substituent of the azo unit; it is typical of the parent azobenzene and usually associated with slower kinetics compared to the other pathways.^{9–11} The rotation is characterized by an out-of-plane motion of the moieties attached to the N=N bond and is typical of azobenzenes decorated with push–pull substituents in polar solvents.⁵ The mechanism is associated with kinetics considerably faster compared to the previous case. The last case is the one involving tautomerism, typical of hydroxy- or amino-substituted azobenzenes.^{12–14} The proton on the OH can be shifted either intra- or intermolecularly on the N=N bond, forming a hydrazone tautomer characterized by an N–NH single bond, around which the substituents can easily rotate and eventually reform the *E*-isomer.^{15,16} While the inversion and rotation mechanisms are monomolecular, the hydrazone

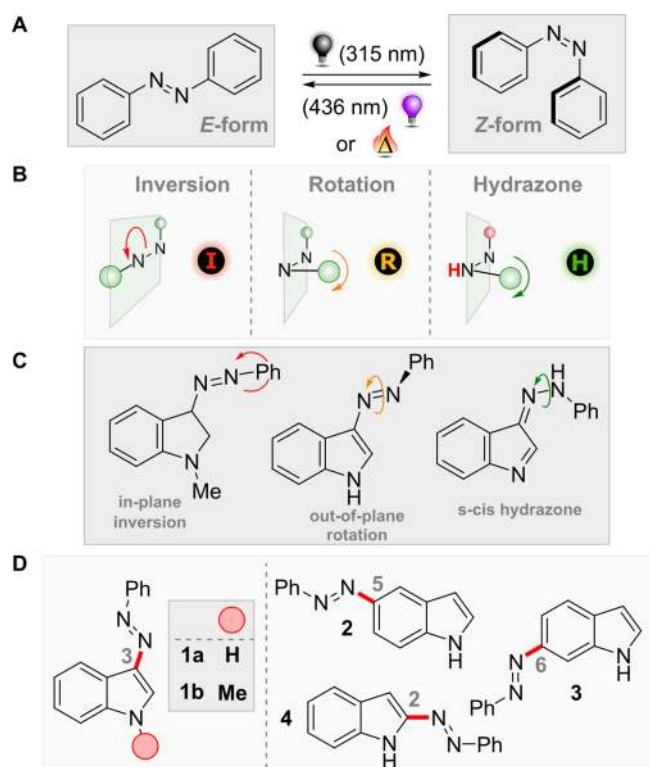
formation can be considered multimolecular as a consequence of the participation of more than one molecule of the substrate to the tautomerism and the assistance of the solvent in the proton transfer.^{17,18} Being able to predict and control the different mechanisms associated with the thermal stability of the *Z*-isomer is vital for planning to use a certain switch for a given application. Indeed, stability ranging from years to months shall be granted for molecular data storage.¹⁹ Moving to the rapidly growing field of photopharmacology, a *Z*-isomer characterized by seconds to months lifetime is usually preferred.²⁰ Finally, extremely unstable *Z*-forms are required for smart materials applications and real-time information transmission (<nanoseconds–seconds).^{15,21} Many strategies have been devised to obtain a precise spatiotemporal control of the thermal *Z*-to-*E* motion of azobenzene,^{16,22} including the use of Brønsted/Lewis acid,^{23–25} electro-,²⁶ and hole catalysis.²⁷

In recent years an increasing number of studies have reported on the discovery and application of heteroaryl azoswitches, e.g., containing the pyridine, imidazole, and pyrazole core.^{28–32} The introduction of a heterocycle in the switch deeply modifies the switching and chemical properties of the molecule, unlocking unique interactive features such as ligand to metal coordination or hydrogen bond formation,

Received: December 5, 2018

Revised: February 6, 2019

Published: February 11, 2019

Chart 1. Isomerization Pathways in (Hetero)azoswitches^a

^aPhotochemical and thermal isomerization of azobenzene (A); pictorial depiction of the different *Z*-to-*E* thermal pathways in azoswitches (B); 3-phenylazaindole transition states schematization of the mechanisms presented in B (C); molecules subject of the current study (D).

without further modification of the core.^{31,33–35} As an added value, the ubiquity of nitrogen heterocycles in chemistry makes the heteroaryl derivatives perfect candidates for future developments of azo-based photoswitches. Indeed, N-heterocycles are used as (organo)catalysts, as ligands in transition metal complexes, and in organic light emitting diodes, they are submoieties in a huge variety of natural compounds, and they can be found in almost 60% of the FDA approved drugs.^{36–40} However, a broader application of heteroaryl azoswitches is only in its beginnings, and consequently, many mechanistic intricacies defining the stability of their *Z*-isomer are not yet resolved. One big limitation is represented by the unpredictable behavior of the heterocycles bearing an NH in the aromatic ring.^{17,41} Although the tunability of the thermal inversion mechanism for their methylated counterparts is reported in two elegant studies,^{31,42} the full understanding of the nature of the thermal isomerization in the NH-containing substrates remains an unresolved challenge.^{31,33,35,43} This often prevented the use of these compounds, favoring the more predictable methylated compounds and leaving the potential of the protonated compounds unexplored,^{31,34} e.g., for non-covalent recognition.⁴⁴ In this framework, we recently contributed to the understanding of the tautomerism mechanism in 3-phenylazaindoles. We found that the modification of the water content in the environment granted nanoseconds–seconds lifetimes to NH-substituted indoles, while methylation of the indolic nitrogen afforded minutes–days lifetimes.¹⁸ The huge variety of τ which can be tuned up to 13 orders of magnitude is presumably a consequence of a

change in mechanism. We reported the presence of an inversion pathway for the methylated compound, a rotation one in the NH-containing compound, in aprotic solvents, and intermolecular hydrazone formation with the NH compounds in protic solvents (Chart 1C).¹⁸ The mechanism variation, and in rare cases coexistence, can be followed by analyzing the kinetics of isomerization and the relative transient spectra.¹⁸

In the present work we focus on the mechanism change in the previously studied phenylazaindole core **1a** and **1b** and extend the number of analyzed structures to 5- (**2**), 6- (**3**), and 2- (**4**) substituted phenylazaindoles (Chart 1D). The spectroscopic and computational data collected for this set of molecules will be used to rationalize how the different substitution patterns influence the choice of mechanism in the azaindole structure, why methylation imposes a change of the isomerization pathway, and when the hydrazone tautomerism can be reasonably claimed to occur.¹⁷ These premises will be subsequently applied to generalize and predict the behavior of an extended selection of heteroaryl azoswitches in their methylated and NH forms.

METHODS

UV/Vis Measurements. An Agilent 8453 spectrometer and a Jasco V-550 spectrometer were employed. The used solvent is stated for each experiment. UV-induced isomerizations were performed through irradiation with a 400 nm Edison Edixeon EDEV-SL-C1-03 (700 mA) LED. The solutions were kept in the dark for 24 h prior the measurements to achieve thermal equilibration.

Thermal *Z*-to-*E*-isomerization was recorded using a Thermo Scientific Multiskan Spectrum (18 °C, see Figure S1). Irradiation prior to measuring was performed using a home-built 96-well plate irradiation setup. A solution of the appropriate arylazaindoles (50 μ M, 250 μ L) was pipetted in a 96-well microtiter plate (Greiner). The wells were covered with a foil to avoid evaporation of the solvent. Then, the plate was irradiated with a 96-wells 365 nm LED irradiation setup for 10 min to ensure that the PSS was reached (Figure S1). The thermal *Z*-to-*E*-isomerization was recorded.

Laser Flash Photolysis. The laser pulse photolysis apparatus consisted of a Flashlamp-pumped Q-switched SpitLight-100 Nd:YAG laser from InnoLas, used at the third harmonic of its fundamental wavelength. It delivered a maximum power of 10 mJ at 355 nm with 3 ns pulse duration. The LP920-K monitor system (supplied by Edinburgh Instruments), arranged in a cross-beam configuration, consisted of a high-intensity 450 W ozone-free Xe arc lamp (operating in pulsed wave), a Czerny-Turner with Triple Grating Turret monochromator, and a five-stage dynode photomultiplier. The signals were captured by means of a Tektronix TDS 3012C digital phosphor oscilloscope, and the data were processed with the L900 software supplied by Edinburgh Instruments. The solutions to be analyzed were placed in a fluorescence cuvette ($d = 10$ mm).

Computational Analysis. All the calculations were carried out at the ω B97X-D/TZVP level. The rotation transition states were treated at the Broken Symmetry (BS)- $U\omega$ B97X-D/TZVP level.

All the optimizations were confirmed to be stationary points by the number of imaginary frequencies found (0 for the minima, 1 for the TSs). The thermochemical data obtained from the frequency calculations were used to compute the free energy of activation of the reactions. The zero-point vibrational

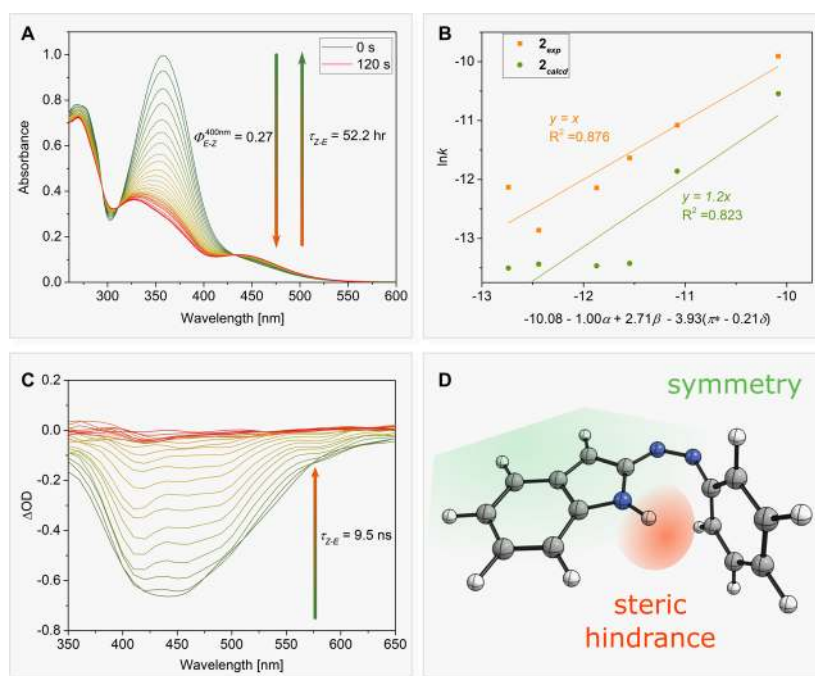


Figure 1. Z-to-E thermal isomerization of compounds **2** and **4**. Time-resolved UV-vis spectrum of compound **2** in DMSO during 120 s of irradiation with an LED ($\lambda = 400$ nm) (A); Kamlet-Taft multivariate regression plot of the experimental and calculated (C-PCM- ω B97X-D/TZVP) Z-to-E $\ln k$ of **2** in the solvents reported in Table 1 (B); transient absorption spectrum of **4** in MeOH (C); computed structure (ω B97X-D/TZVP level) of the Z-isomer of **4** (D).

Table 1. Lifetimes for the Z-to-E Thermal Isomerization of Compounds 1–4

solvent	lifetimes (τ) [s]				
	1a ¹⁸	1b ¹⁸	2	3	4
cyclohexane	4.25×10^{-2}	3.96×10^4	2.01×10^4	1.19×10^4	7.7×10^{-9}
toluene	4.75×10^{-2}	1.03×10^4	6.48×10^4	2.45×10^4	8.3×10^{-9}
MeCN	4.30×10^0	1.04×10^5	3.85×10^5	1.43×10^5	9.2×10^{-9}
MeOH	6.80×10^{-3}	8.64×10^4	1.13×10^5	4.97×10^4	9.5×10^{-9}
DMSO	6.50×10^0	2.25×10^5	1.88×10^5	2.95×10^5	9.3×10^{-9}
DMSO-water (1:1)	1.88×10^{-4}		1.86×10^5	4.03×10^4	1.1×10^{-8}

energy was always added to the G values obtained from the frequency calculations. All the isodesmic equations considered in this study were obtained subtracting the sum of the free energies and ZVPE of the reagents to the one of the products of the reaction.

RESULTS AND DISCUSSION

Thermal Isomerization in Differently Substituted Phenylazindoles: Isomerization of Compounds 2–4.

Compounds **2**, **3**, and **4** were synthesized from the corresponding amino indoles in a reaction with nitrosobenzene following the Baeyer-Mills protocol (see Scheme S1). Compounds **2** and **3** are particularly interesting because the azo function is attached to the benzene moiety of the indole core. They allow the study of the behavior of bicyclic heteroaryl azoswitches substituted on the homocyclic part. We triggered the formation of the Z-isomer by irradiation of a 50 μ M solution of the compound in different solvents with a 400 nm LED (Figure 1A). The values of quantum yields of E-to-Z isomerization ($\Phi_{E-Z} \sim 0.3$ in all the solvents studied) are similar to the ones reported for electron-rich substituted azobenzenes (see Table S1).¹ Compound **3** affords photostationary distributions (PSDs) containing $\geq 80\%$ of Z-isomer at

the photostationary state (PSS), while the Z-form in compound **2** is less abundant ($50\% < \text{PSD} < 76\%$, see Table S1). We could not analyze the photostationary distribution of compound **4** due to its short lifetimes of Z-to-E conversion.

The thermal Z-to-E relaxation process was studied in the same solvents and solvent mixtures (Table 1). Both **2** and **3** exhibit lifetimes in the range of several hours to a few days, resembling the behavior of the methylated compound **1b**.¹⁸ In contrast, the parent compound **1a** relaxes in seconds or much faster from the PSS to the thermodynamic equilibrium. Besides, 5-phenylazindole (**2**) exhibits two to four times greater τ than the corresponding 6-phenylazo derivative (**3**) in all investigated solvents. We applied a variation of the Kamlet and Taft linear solvation energy relationship (LSER) (Figure 1B) to examine the presence of a trend in the lifetimes.⁴⁵ This method allows to quantitatively describe the specific (electron-pair sharing) and nonspecific (polarity) effects of the solvents on the rate of the reaction (more details in the Supporting Information, in section 3.1.3). From the multivariate analysis it appeared that the polarity (π^*) of the medium has the most significant effect in lowering the rate of thermal isomerization of **2** and **3**, while the basicity (β) of the solvent (and consequently the formation of a hydrogen bond interaction)

has an opposite role for **2** (Figure 1B, for **3**, see Figure S26). These considerations are in line with previous reports of an inversion transition state (see Chart 1B), supporting the presence of this specific mechanism in the thermal isomerization of compounds **2** and **3**.^{5,35}

Indeed, plotting the computed values of the thermal isomerization rates obtained considering an inversion pathway versus the same multivariate function furnished a slope that is comparable with the experimental values (Figure 1B, in green). The simulated energies were obtained as Boltzmann-factor-weighted averages between the isomerization of the two more stable conformers at the C-PCM- ω B97X-D/TZVP level of theory (section 6.2 of the Supporting Information). Having the computed ΔG^\ddagger in hand, we obtained the simulated kinetic constants applying the Eyring equation. It has to be noted that the computed values of $\ln k$ slightly suffer in accuracy, probably due to the oversimplification of the solvent medium as a dipolar continuum. It is known that an explicit solvent molecule modifies the calculated $\ln k$ significantly without a change in the mechanism type due to the interaction with the indolic NH.³⁵ However, we consider the choice of functional, basis set, and solvent method precise in predicting the same trend we found experimentally.

In general, the behavior of **2** and **3** resembles the one reported for electron-rich azobenzenes and *N*-methylated heterocyclic azo compounds like **1b** or recently reported methylated imidazole and pyrazole derivatives.^{31,35,46}

Compound **4** represents the other side of the coin, showing some of the shortest lifetimes for *Z*-to-*E* thermal isomerization registered for a neutral azo compound (only push-pull systems bearing pyridinium salts have reached the subnanosecond range in azoswitches so far).^{15,18,29,47} All of the τ oscillate around the 10 ns scale, with minimal or no solvent effect (see Table 1 and Figure 1C). The presence of a hydrazone intermediate is recurrently mentioned as the leading actor of the thermal instability of the *Z*-form of heteroaryl azobenzenes;^{17,29} however, it was not observed in our experiments. The geometry of *Z*-**4**, with the phenyl ring “shielding” the NH and hindering the site from the solvent, explains the limited solvent effect in the thermal *Z*-to-*E* isomerization rates of **4** (see Figure 1D). The mechanism of thermal isomerization is the rotation as determined by calculations, exactly like in compound **1a** in the absence of a protic environment.¹⁸

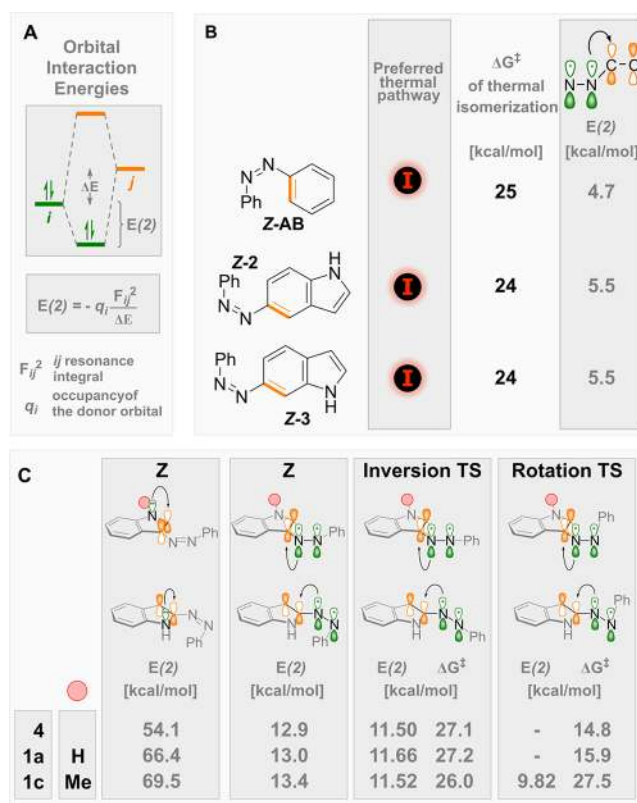
Moreover, it was not possible to detect the formation of the $n \rightarrow \pi^*$ transition typical of the appearance of the *Z*-isomer.¹⁸ The explanation probably lies in the symmetry of the preferred conformation of *Z*-**4**, which does not allow this specific transition to appear (see Figure 1D, cf. also the calculated absorption spectrum of *Z*-**4** in section 6.5 in the Supporting Information). A similar situation was found for compound **1a** in aprotic solvents.¹⁸

Rationalization of the Monomolecular Thermal Isomerization Mechanisms in 1–4. The monomolecular thermal behavior of the differently substituted indoles is extremely peculiar in its variety. Attaching the azo moiety to the homocyclic side of the indole always affords an inversion mechanism (compounds **2**, **3**), while positioning the N=N in position 2- (compound **4**) grants a rotation pathway associated with ultrafast isomerization rates, regardless of the solvent of choice. 3-Phenylazaindoles, on the other hand, are reported to isomerize either via rotation (**1a**, in the absence of protic solvent)¹⁸ or via inversion (if methylated like **1b**).¹⁸ These

experimental findings were computationally confirmed at the BS- ω B97X-D/TZVP^{18,32} level of theory, analyzing the nature of the different transition states.

We found that the NBO (natural bond orbital) analysis of specific orbital interactions in the *Z*-isomer of the azaindoles offers a simplified, yet chemically appropriate way to understand the thermal pathway chosen by a given structure.^{31,48} The bond orders obtained from this method were already used to correlate the thermal stability of a set of methylated *Z*-isomers of heteroaryl photoswitches.³¹ The NBO package furnishes also a second-order perturbative approach (Chart 2A) which estimates the stabilization energy ($E(2)$)

Chart 2. Theoretical Analysis of the Monomolecular Mechanisms in Compounds 1–4^a



^aPictorial representation of the stabilization energy ($E(2)$) between a filled (*i*) and empty (*j*) orbital in a molecule (A); ΔG^\ddagger of inversion and main orbital interactions found in compounds *Z*-**2**, **3** compared to *Z*-azobenzene *Z*-**AB**. In the figure, the empty π^* orbital considered for second-order interaction with the N=N is highlighted in yellow (B); pictorial representation of the isodesmic reactions considered for compounds **1a**, **b** and **4** (C); main orbital interactions found in compounds **1a**, **c** and **4** in their *Z*-form, inversion, and rotation transition state. The ΔG^\ddagger (BS- ω B97X-D/TZVP) for each respective transition state is reported.

granted by the delocalization of the electrons belonging to a filled Lewis-localized orbital in the molecule (*i*, depicted in green in Chart 2) into an empty one (*j*, in yellow).^{49–51} This approach in the analysis of the wave function furnishes useful hints on the specific interactions stabilizing a structure and the related energies. Interestingly, if we consider the energy gain between the filled N=N and the neighboring empty double bond on the indole (Chart 2B), the $E(2)$ values are slightly bigger compared to the reference azobenzene (*Z*-**AB**, Chart

2B). As a first approximation, we can conclude that given the more significant stabilization interactions, *Z*-2 and *Z*-3 prefer to isomerize via the inversion pathway typical of unsubstituted azobenzene back to the *E*-form.¹ The inversion transition structure does not disrupt the conjugation between the (heterocyclic) ring and the N=N bond, in contrast to the rotation transition state (where the N=N π bond is completely broken due to a 90° dihedral angle with the substituents, see Chart 1B). Hence, a system having a stronger delocalization (a larger $E(2)$) prefers to maintain that interaction also in the transition structure, instead of breaking it via a rotation pathway. The $E(2)$ values do not correlate directly with the computed ΔG^\ddagger because they consider only the interactions at the minimum energy of the *Z*-isomer. However, they furnish a qualitative indication that can be used to choose the right mechanism of isomerization, which quantitatively affords lower barriers compared to *Z*-AB (see Chart 2B), as expected from structures that electronically resemble an electron-rich azobenzene.¹

Moving to compounds **1a**, **b** and **4**, the nonmethylated compounds have low TS energies for thermal isomerization due to a rotation pathway (see the ΔG^\ddagger values reported in Chart 2C) The N-methylated compound **1b**, on the other hand, prefers an inversion pathway to the rotational one, with a barrier ca. 10 kcal mol⁻¹ higher with respect to compound **1a**.¹⁸ The reason can again be found in the orbital interactions. In particular, methylation rises the energy of the filled lone-pair orbital on the N (two C–H σ bonds of the methyl have a filled–filled destabilizing interaction of ca. 8 kcal mol⁻¹ with the lone pair on N). This effect correlates directly with the $E(2)$ values of donor–acceptor stabilization between the n orbital on the N and the π^* orbital on the C2–C3 carbons of the indole ($n_{(N)} \rightarrow \pi^*_{(CC)}$ values in Chart 2C, on the right). The direct consequence of this delocalization is the change in energy of the above $\pi^*_{(CC)}$ that can now interact in a stronger fashion with $\pi_{(NN)}$ in *Z*-**1b**, compared with **1a** and **4**. The interactions of the N=N bond with the neighboring empty C=C in the *Z*-isomer can explain a change of mechanism. Compound **1b** is less prone to weaken (and ultimately nullify) these stabilizing orbital contributions following an inversion transition state. The effect of the substitution can be followed analyzing the same orbital interactions in the transition state. Indeed, in **1a** and **4** no $\pi_{(NN)} \rightarrow \pi^*_{(CC)}$ is present anymore. On the contrary, in **1b** where this interaction is more pronounced in the ground state of the *Z*-isomer, it is only slightly weakened in the rotation TS. As expected this transition state is high in energy, due to the persistence of the N=N double bond character, which is not prone to rotation. Hence in **1b** the system prefers to isomerize thermally via an inversion transition state, where the $\pi_{(NN)} \rightarrow \pi^*_{(CC)}$ is more intense due to the better geometrical disposition of the transition structure.

A broader treatment considering different substitution patterns, viz., 2-methyl-3-phenylazindole, the explicit effect of different solvents on the N lone pair, and the isodesmic reactions associated with their *Z*-forms and TSs are presented in section 6.4 in the Supporting Information.

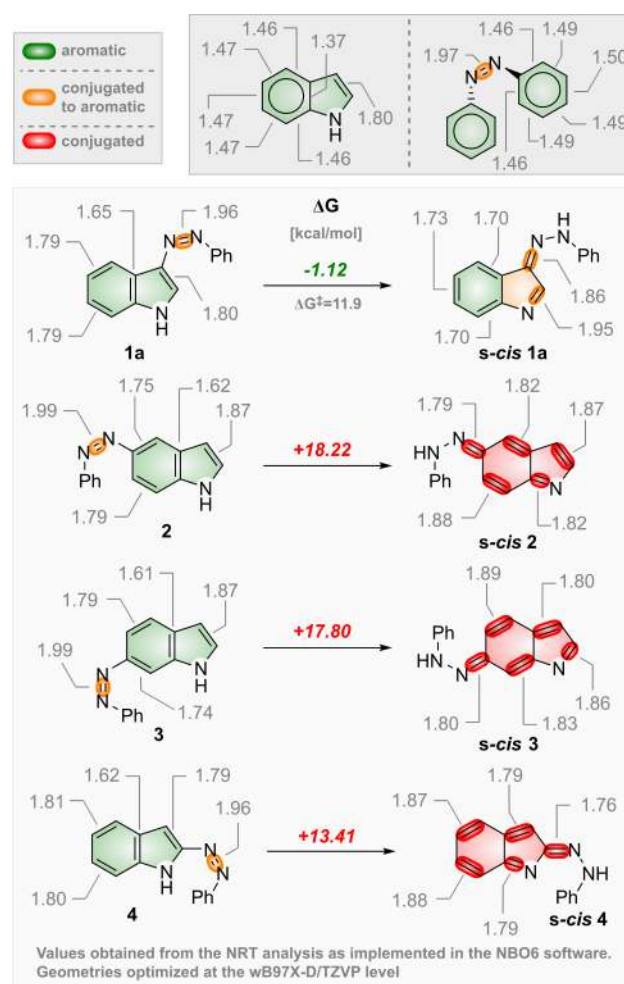
Feasibility of the Hydrazone Tautomerism in Compounds 1–3. In our previous study, we observed that the proton availability in the solvent mixture is crucial for the rate of the *Z*-to-*E* relaxation as it facilitates isomerization via the intermolecular hydrazone pathway.¹⁸ However, from the results reported in Table 1 it appears that **1a** is subject to a

steep increase in the *Z*-to-*E* thermal reaction rate in the presence of a protic environment. To reinforce this hypothesis, we studied the isomerization of the *Z*-form of compounds **2**, **3**, and **4** in a DMSO–water 1:1 solution in the presence of DBU (1,5-diazabicyclo(5.4.0)undec-7-ene). Addition of DBU of the thermal reaction in **1a** decreased to the nanosecond range;¹⁸ however, it did not exert a substantial difference in the *Z*-form conversion for compounds **2–4**.

Indeed, the optimization of the intermolecular transition state **1a** in the presence of explicit molecules of solvent for the proton transfer leading to the hydrazone is feasible ($\Delta G = +11.9$ kcal/mol at the BS- ω B97X-D/TZVP level, see the Supporting Information).¹⁸ On the other hand, the same calculations for compounds **2–4** could not reach convergence. The reason for this discrimination relates to the high energy (ΔG) of formation of the hydrazone in compounds **2**, **3**, and **4** compared to **1a** (–1.12 kcal/mol for **1a** versus ca. +13–18 kcal/mol, see Chart 3).

Seeking a correlation between the feasibility of the hydrazone tautomerism and the structure of the *Z*-form, we again decided to use the NBO analysis. We studied the bond

Chart 3. Hydrazone Mechanism Feasibility in Compounds 1–4^a



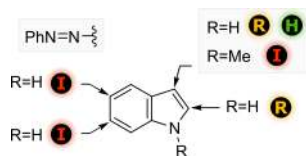
^a ΔG of the simplified tautomerism reaction of compounds **1–4**. The bond orders calculated with the natural resonance theory approach are given for each Lewis-localized double bond. In the inset, the reference values for indole and azobenzene are reported.

orders in the *Z*-forms and the respective *s*-cis hydrazone forms of the molecules, as obtained by applying the natural resonance theory analysis (NRT) present in the NBO package. NRT describes the bonding accurately in highly delocalized molecules, such as the azoindoles. Moreover, it represents the molecular connectivity as a sum of weighted structures that are consistent with the qualitative, and chemically more familiar, Pauling–Wheland resonance theory.⁴⁹

The substitution with an azo group localizes the double bonds on the heterocyclic ring in the *Z*-isomers, compared to the unfunctionalized indole itself (indeed a resonance structure in the *Z*-form weights more than the others, see section 6.1.1 in the Supporting Information; compare the *Z*-isomers in Chart 3 with the unfunctionalized indole in the inset). The tautomerism leads to a gain in energy only for the formation of *s*-cis **1a**, maintaining the aromaticity in the homocyclic part of the indole (and slightly strengthening it: cf. the lower bond orders in the homocycle in *s*-cis-**1a**, indicating a greater delocalization). In all the other examples the aromaticity is completely lost with the formation of quinoid-like structures (Chart 3). The same considerations can be derived, albeit less intuitively, studying the shapes of the HOMO and HOMO–1 orbitals in the hydrazone forms (see section 6.3 in the Supporting Information and Figures S97–100).

Generalization of the Thermal Isomerization in Azoindoles. From our analysis of the mono- and multi-molecular (namely the tautomerism) mechanisms, we can derive a generalization of the thermal isomerization behavior in azoindoles (see Chart 4). The functionalization of the indole

Chart 4. Generalization of the *Z*-to-*E* Thermal Mechanisms in Azoindoles^a



^aThe figure represents the different mechanisms (inversion, rotation, and hydrazone formation) possible for the different substitution patterns analyzed.

with the azo group on the phenyl side (**2**, **3**) leads to switches similar to electron-rich azobenzenes. The primary mechanism of *Z*-to-*E* conversion is the in-plane inversion, regardless of the presence of an NH free moiety. The molecule preferentially follows an inversion TS to minimize the loss of conjugation between the azo group and the heterocycle. The same concepts extend to the methylated molecule **1b**. The orbital interactions between the indole and the azo group can be weakened by removing the methyl affording **1a** that, in the absence of protic solvents, is characterized by a *Z*-to-*E* rotation mechanism. The intramolecular interaction between an explicit molecule of proton-accepting solvent and the NH can be used to tune the rotation mechanism further (see Table 1) and in a more in-depth theoretical treatment in section 6.4 of the Supporting Information. Attaching the N=N core in position 2- (**4**), on the other hand, grants unstable PSS upon irradiation, with extremely fast thermal back-isomerization lifetimes. The main pathway proceeds through a low-energy rotational TS.

The viability of the hydrazone pathway in NH-containing switches can be tested comparing the energy difference (ΔG) between the *Z*-isomer and the respective *s*-cis hydrazone. If the

value is greater than 10 kcal mol⁻¹, we can exclude the tautomerism to occur, the ΔG of formation being comparable with (and the related ΔG^\ddagger greater than) the ΔG^\ddagger of other monomolecular rotation. Only in **1a** can the hydrazone pathway be triggered using a protic solvent due to the energetically favored formation of the tautomer. This pathway is not feasible for compounds **2**, **3**, and **4** due to the loss of aromaticity in the *s*-cis hydrazone. Indeed, the joint spectroscopic and computational investigation furnished a way to discriminate the rotational and hydrazone pathway, even in the astonishingly fast *Z*-to-*E* isomerizing compound **4**.

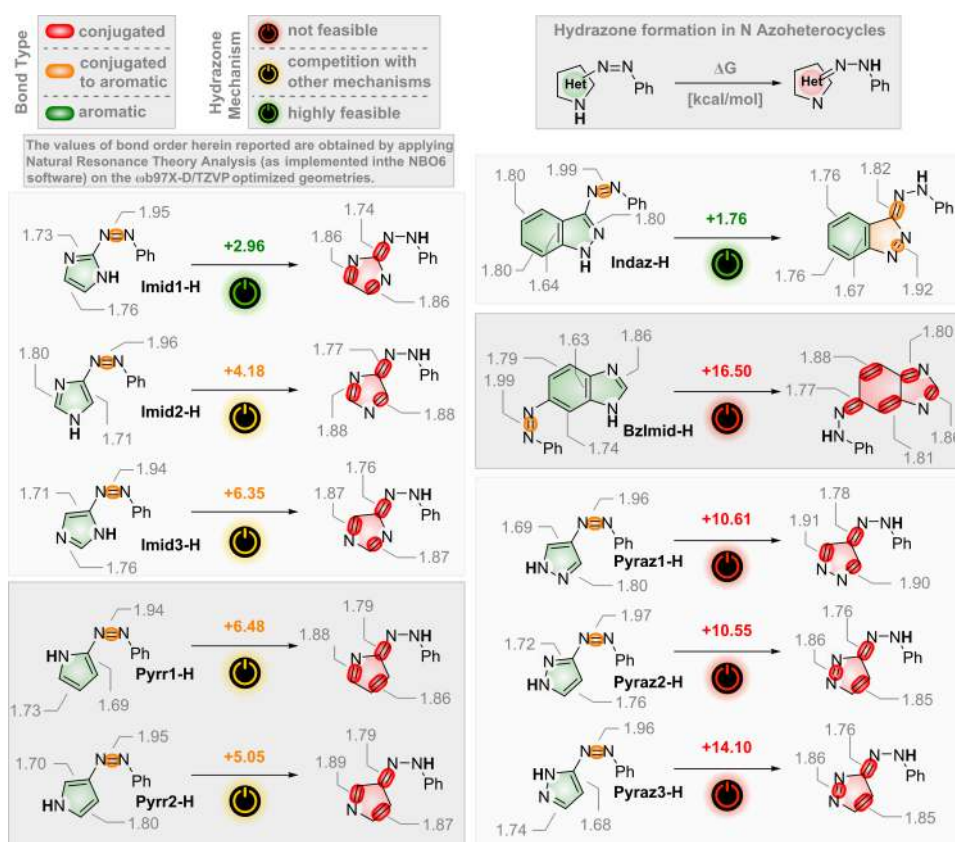
Generalization of the *Z*-to-*E* Thermal Isomerization in Azoheteroarenes. We decided to extend these concepts to a series of azoswitches differently substituted with heterocyclic cores (Charts 5 and 6), namely imidazole (Imid1–3), pyrrole (Pyr1–2), indazole (Indaz), benzimidazole (Bzimid), and pyrazole (Pyr1–3). Both the unsubstituted (dubbed with a -H) and the methylated (dubbed with a -Me) forms were computationally studied in their thermal *Z*-to-*E* reaction course, comparing our calculated data with the experimental ones already present in the literature. Only Pyr2-H and Pyr3-H were not studied as photoswitches so far.³¹

We applied the same approach the indoles to study the viability of the hydrazone tautomerism (see Chart 5). As an empiric rule of thumb based on the azoindoles, we considered that the protic exchange equilibrium can be highly feasible with hydrazones characterized by ΔG of formation <+3 kcal mol⁻¹. Imid1-H and Indaz-H belong to this category; the latter resembles the case of **1a** with a partial loss of aromaticity. As the azoindole **1a**, Indaz-H possesses very low ΔG values. We considered the tautomerism probable for ΔG ca. +5–6 kcal mol⁻¹, although, if present, in competition with other monomolecular isomerization pathways. This class is represented by Imidazoles Imid2,3-H and pyrroles. Finally, we considered ΔG values >+10 kcal mol⁻¹ too high for the hydrazone equilibrium to occur. Benzimidazoles, which form quinoid-like structures as **2**, **3** and pyrazoles, behave accordingly.

As expected, the five-membered heterocycles possessing lower aromaticity are more prone to tautomerize (the aromaticity follows the following scale: imidazoles ~ pyrrole < pyrazole⁵²).

Starting from these premises we summarize in Chart 6 the main orbital contributions in the azaheterocycles, viz., the $\pi_{(NN)} \rightarrow \pi^*_{(XY)}$ (with X = Y the π bond of the heterocycle attached to the N=N) and two $n_{(N)} \rightarrow \pi^*_{(\alpha\beta)}$ (with $\alpha = \beta$ the π bonds conjugated with the NH or NMe lone pair, in yellow the one directly attached to the heterocycle, in red the other one). Refer to Figure S224 for a broader set of data. The methylated imidazoles are reported to be relatively stable in their methylated form, and the barriers calculated for the in-plane *Z*-to-*E* inversion pathway match the experimental values.^{17,46} The unsubstituted forms, on the other hand, show faster isomerization rates ascribed to a rotation TS, in the absence of protic solvent, or to the presence of hydrazone tautomerism when protic environment is present. The diminished orbital interactions found are coherent with the change of monomolecular mechanism. Indeed, this reasoning can explain the well-documented reactivity in different solvents of the unsubstituted and methylated Imid1³⁹ and the less investigated Imid2-H and Imid3-H. The same considerations can be extended to the pyrroles^{31,53} and indazole. Indaz

Chart 5. Feasibility of the Hydrazone Mechanism in Differently Substituted Azaheterocycles ΔG Of the Simplified Tautomerism Reaction of Different Heterocyclic Azocompounds^a



^aThe bond orders calculated with the natural resonance theory approach are given for each Lewis-localized double bond.

represents a striking case on how methylation (or in general N-substitution) can profoundly influence the thermal reactivity of heteroaryl azoswitches. **Indaz-H** is reported to have subnanosecond *Z*-to-*E* τ in protic medium,⁴⁷ probably due to hydrazone tautomerism, according to our model. On the other hand, the alkylated form is characterized by lifetimes in the hour range (or in the days if aromatic substituents are placed on the N).³²

The behavior of **Bzimid** is similar to the one of **2** and **3**, where the azo group is positioned on the homocyclic side of the heterocycle. Despite the presence of an unsubstituted NH in the structure, both the calculations and the experimental data confirm the choice of an inversion thermal pathway.^{54,55}

Furthermore, our approximation can be used to explain the otherwise unpredictable behavior of the pyrazoles. The **Pyraz1-3-Me** were thoroughly studied and well characterized in their inversion *Z*-to-*E* mechanism, while in the same studies the unsubstituted derivatives were not investigated, deeming the *Z*-isomer unstable for the presence of the NH.^{31,42} Very recently, a study on **Pyraz1-H** confuted this theory, reporting switches with the τ in the hour range.³⁵ This result is in accordance with the results derived from our method, which exclude the viability of the hydrazone tautomerism in this particular case and predict an inversion mechanism for *Z*-**Pyraz1-H**. Indeed, this molecule is the only one in which the $\pi_{(NN)} \rightarrow \pi^*_{(XY)}$ exactly match in both the methylated and unsubstituted *Z*-forms, probably due to a very high contribution in the $n_{(N)} \rightarrow \pi^*_{(\alpha\beta)}$ interactions (see Chart 6). **Pyraz2-H** and **Pyraz3-H** are predicted to undergo only an

inversion (for the first, that possesses a $\pi_{(NN)} \rightarrow \pi^*_{(XY)}$ greater than **Pyraz2-Me**) and a rotation mechanism (for the later), with no possible hydrazone tautomerism. More thorough investigations on **Pyraz2-H** and **Pyraz3-H** will be content of our future work.

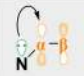
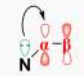



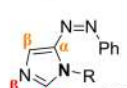
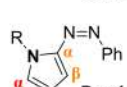
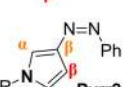
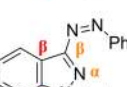
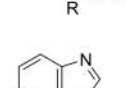
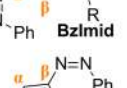
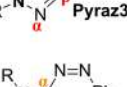

CONCLUSIONS

In summary, we investigated a small series of phenylazoindoles, bearing the azo function on different positions of the indole core, using a combined spectroscopic and computational approach. These results allowed to rationalize a series of criteria able to discriminate both the type of monomolecular thermal *Z*-to-*E* pathway and the possibility of the hydrazone tautomerism in protic environment. The computational approach based on natural bond orbitals and natural resonance theory was followed, granting a better understanding of the factors behind the choice of the different mechanisms.

The approximations we considered were extended to a series of azoheterocycles, namely azo-imidazoles, benzimidazole, pyrroles, pyrazoles, and indazole, both in their unsubstituted and N-methylated forms. The calculations were found to be consistent with the experimental data regarding the thermal behavior of the *Z*-isomer of the heterocycles above. Hence, we can conclude then that the approach based on the NBO analysis we followed can be used to predict the general thermal behavior of a class of heterocyclic azoswitches, based on their substitution pattern.

Albeit no attempt was made to analyze the effect of more electronically complex substituents on the switch, which has to

Chart 6. Generalization of the Thermal Z-to-E Isomerization in Different Heterocycles^a

	R	τ Reference	Preferred thermal pathway	ΔG^\ddagger [kcal/mol]			
					[kcal/mol]	[kcal/mol]	[kcal/mol]
	H	100 s Ref. 35	R H	15.8	72.9	56.8	16.55
	Me	9 hrs Ref. 35	I	20.8	74.9	59.3	16.64
	H	^a Ref. 35	R H	17.6	58.2	65.7	13.64
	Me	3.5 days Ref. 29	I	25.5	60.4	68.2	13.67
	H	^a Ref. 42	R H	16.4	49.5	82.0	14.05
	Me	6.5 days Ref. 29	I	24.8	50.2	86.7	14.04
	H	^a Ref. 48	R H	9.0	55.8	66.6	14.16
	Me	17 hrs Ref. 29	I	22.4	56.2	70.1	14.20
	H	^a Ref. 48	R H	18.4	65.3	52.0	12.01
	Me	5.3 day Ref. 29	I	25.2	67.9	53.6	12.09
	H	< ns Ref. 43	R H	13.3	58.5	54.4	15.91
	Me	19 hrs Ref. 43	I	20.3	62.4	56.4	15.95
	H	< 2 weeks Ref. 49	I	24.0			5.26
	Me	> 3 hrs Ref. 50	I	24.4			5.65
	H	2 hrs Ref. 33	I	27.1	74.5	47.2	13.37
	Me	>1400 days Ref. 29	I	27.6	77.4	47.3	13.37
	H	b	I	27.6	65.0	60.6	14.60
	Me	16 days Ref. 29	I	26.0	66.2	63.7	14.55
	H	b	R	17.9	59.9	61.2	14.00
	Me	>106 days Ref. 29	I	26.1	62.8	62.9	14.12

a: "fast isomerization"; b: not known.

^aFor each heterocyclic structure, the thermal lifetime (wherever present) is cited. The preferred isomerization pathway is given as R (rotation), H (hydrazone), or I (inversion). The ΔG^\ddagger of the monomolecular pathway is reported (hence, when more than one thermal mechanism is viable, namely, both rotation and inversion, only the rotation TS free energy of activation is reported). The main $E(2)$ considered for the analysis are also furnished.

be treated as individual cases for each heterocycle, we were able to derive a series of chemically intuitive approaches that can be relevant in the de novo design of new scaffolds. In particular, the NRT analysis on the Z-form of the switch is useful to estimate the feasibility of the hydrazone tautomerism, according to product and reagent electronic distributions. Moreover, the NBO analysis of the Z-isomer reveals the electronic nature of the thermal stability of a structure. We are confident these findings will be useful to broaden in number and applicability the class of heterocyclic-substituted azoswitches.

■ ASSOCIATED CONTENT

📄 Supporting Information

The Supporting Information is available free of charge on the ACS Publications website at DOI: 10.1021/acs.jpca.8b11734.

General information, synthetic procedures, spectroscopic analysis, NMR spectra, HPLC traces, and computational analysis (PDF)

■ AUTHOR INFORMATION

Corresponding Authors

*E-mail: fagnoni@unipv.it.

*E-mail: burkhard.koenig@chemie.uni-regensburg.de.

ORCID

Burkhard König: 0000-0002-6131-4850

Notes

The authors declare no competing financial interest.

ACKNOWLEDGMENTS

We thank the Consortium CINECA-SCAI for the computational hours granted (project HP10C8U1NY). N.A.S. thanks the Studienstiftung des Deutschen Volkes for a Ph.D. scholarship. A.B. thanks B. Sammartino for inspiration for the work, while S.C. thanks Dr. Davide Ravelli for fruitful discussions.

REFERENCES

- (1) Bandara, H. M. D.; Burdette, S. C. Photoisomerization in Different Classes of Azobenzene. *Chem. Soc. Rev.* **2012**, *41*, 1809–1825.
- (2) *Molecular Switches*; Feringa, B. L., Browne, W. R., Eds.; Wiley-VCH Verlag GmbH & Co. KGaA: Weinheim, Germany, 2011.
- (3) Hartley, G. S. The Cis-Form of Azobenzene. *Nature* **1937**, *140*, 281.
- (4) Liu, X.-M.; Jin, X.-Y.; Zhang, Z.-X.; Wang, J.; Bai, F.-Q. Theoretical Study on the Reaction Mechanism of the Thermal Cis – Trans Isomerization of Fluorine-Substituted Azobenzene Derivatives. *RSC Adv.* **2018**, *8*, 11580–11588.
- (5) Dokić, J.; Gothe, M.; Wirth, J.; Peters, M. V.; Schwarz, J.; Hecht, S.; Saalfrank, P. Quantum Chemical Investigation of Thermal Cis-to-Trans Isomerization of Azobenzene Derivatives: Substituent Effects, Solvent Effects, and Comparison to Experimental Data. *J. Phys. Chem. A* **2009**, *113*, 6763–6773.
- (6) Conti, I.; Garavelli, M.; Orlandi, G. The Different Photoisomerization Efficiency of Azobenzene in the Lowest $N\pi^*$ and $\Pi\pi^*$ Singlets: The Role of a Phantom State. *J. Am. Chem. Soc.* **2008**, *130*, 5216–5230.
- (7) Muždalo, A.; Saalfrank, P.; Vreede, J.; Santer, M. Cis -to- Trans Isomerization of Azobenzene Derivatives Studied with Transition Path Sampling and Quantum Mechanical/Molecular Mechanical Molecular Dynamics. *J. Chem. Theory Comput.* **2018**, *14*, 2042–2051.
- (8) Merino, E.; Ribagorda, M. Control over Molecular Motion Using the Cis – Trans Photoisomerization of the Azo Group. *Beilstein J. Org. Chem.* **2012**, *8*, 1071–1090.
- (9) Asano, T.; Okada, T.; Shinkai, S.; Shigematsu, K.; Kusano, Y.; Manabe, O. Temperature and Pressure Dependences of Thermal Cis-to-Trans Isomerization of Azobenzenes Which Evidence an Inversion Mechanism. *J. Am. Chem. Soc.* **1981**, *103*, 5161–5165.
- (10) Kawachi, S.; Imase, T.; Tamura, Y.; Watanabe, J. Transition State Structures of Thermal Cis-Trans Isomerization Reaction of Azobenzenes. *Mol. Cryst. Liq. Cryst. Sci. Technol., Sect. A* **2000**, *345*, 69–74.
- (11) Ikegami, T.; Kurita, N.; Sekino, H.; Ishikawa, Y. Mechanism of Cis-to-Trans Isomerization of Azobenzene: Direct MD Study. *J. Phys. Chem. A* **2003**, *107*, 4555–4562.
- (12) Matazo, D. R. C.; Ando, R. A.; Borin, A. C.; Santos, P. S. Azo-Hydrazone Tautomerism in Protonated Aminoazobenzenes: Resonance Raman Spectroscopy and Quantum-Chemical Calculations. *J. Phys. Chem. A* **2008**, *112*, 4437–4443.
- (13) Garcia-Amorós, J.; Sánchez-Ferrer, A.; Massad, W. A.; Nonell, S.; Velasco, D. Kinetic Study of the Fast Thermal Cis-to-Trans Isomerisation of Para-, Ortho- and Polyhydroxyazobenzenes. *Phys. Chem. Chem. Phys.* **2010**, *12*, 13238–13242.
- (14) Poutanen, M.; Ahmed, Z.; Rautkari, L.; Ikkala, O.; Priimagi, A. Thermal Isomerization of Hydroxyazobenzenes as a Platform for Vapor Sensing. *ACS Macro Lett.* **2018**, *7*, 381–386.
- (15) Garcia-Amorós, J.; Cuadrado, A.; Reig, M.; De Waele, V.; Poizat, O.; Velasco, D. Spatially Close Azo Dyes with Sub-Nanosecond Switching Speeds and Exceptional Temporal Resolution. *Chem. - Eur. J.* **2015**, *21*, 14292–14296.
- (16) Garcia-Amorós, J.; Velasco, D. Recent Advances towards Azobenzene-Based Light-Driven Real-Time Information-Transmitting Materials. *Beilstein J. Org. Chem.* **2012**, *8*, 1003–1017.
- (17) Otsuki, J.; Suwa, K.; Sarker, K. K.; Sinha, C. Photoisomerization and Thermal Isomerization of Arylazoimidazoles. *J. Phys. Chem. A* **2007**, *111*, 1403–1409.
- (18) Simeth, N. A.; Crespi, S.; Fagnoni, M.; König, B. Tuning the Thermal Isomerization of Phenylazindole Photoswitches from Days to Nanoseconds. *J. Am. Chem. Soc.* **2018**, *140*, 2940–2946.
- (19) Sauer, M. Reversible Molecular Photoswitches: A Key Technology for Nanoscience and Fluorescence Imaging. *Proc. Natl. Acad. Sci. U. S. A.* **2005**, *102*, 9433–9434.
- (20) Velema, W. A.; Szymanski, W.; Feringa, B. L. Photopharmacology: Beyond Proof of Principle. *J. Am. Chem. Soc.* **2014**, *136*, 2178–2191.
- (21) Gelebart, A. H.; Jan Mulder, D.; Varga, M.; Konya, A.; Vantomme, G.; Meijer, E. W.; Selinger, R. L. B.; Broer, D. J. Making Waves in a Photoactive Polymer Film. *Nature* **2017**, *546*, 632–636.
- (22) Bléger, D.; Schwarz, J.; Brouwer, A. M.; Hecht, S. O -Fluoroazobenzenes as Readily Synthesized Photoswitches Offering Nearly Quantitative Two-Way Isomerization with Visible Light. *J. Am. Chem. Soc.* **2012**, *134*, 20597–20600.
- (23) Schulte-Frohlinde, D. Über den Mechanismus der Katalytischen Cis → Trans-umlagerung von Azobenzol. *Justus Liebigs Ann. Chem.* **1958**, *612*, 131–138.
- (24) Arnaud, R.; Lemaire, J. Isomérisation Cis – Trans de l'azobenzène Catalysée Par l'iode. III. *Can. J. Chem.* **1974**, *52*, 1868–1871.
- (25) Hall, C. D.; Beer, P. D. Trico-Ordinate Phosphorus Compounds as Catalysts for the Isomerization of (Z)-to (E)-Azobenzene. *J. Chem. Soc., Perkin Trans. 2* **1991**, *12*, 1947–1950.
- (26) Goulet-Hanssens, A.; Utecht, M.; Mutruc, D.; Titov, E.; Schwarz, J.; Grubert, L.; Bléger, D.; Saalfrank, P.; Hecht, S. Electrocatalytic Z → E Isomerization of Azobenzenes. *J. Am. Chem. Soc.* **2017**, *139*, 335–341.
- (27) Goulet-Hanssens, A.; Rietze, C.; Titov, E.; Abdullahu, L.; Grubert, L.; Saalfrank, P.; Hecht, S. Hole Catalysis as a General Mechanism for Efficient and Wavelength-Independent Z → E Azobenzene Isomerization. *Chem.* **2018**, *4*, 1740–1755.
- (28) Wang, Y.-T.; Liu, X.-Y.; Cui, G.; Fang, W.-H.; Thiel, W. Photoisomerization of Arylazopyrazole Photoswitches: Stereospecific Excited-State Relaxation. *Angew. Chem., Int. Ed.* **2016**, *55*, 14009–14013.
- (29) Garcia-Amorós, J.; Díaz-Lobo, M.; Nonell, S.; Velasco, D. Fastest Thermal Isomerization of an Azobenzene for Nanosecond Photoswitching Applications under Physiological Conditions. *Angew. Chem., Int. Ed.* **2012**, *51*, 12820–12823.
- (30) Venkataramani, S.; Jana, U.; Dommaschk, M.; Sonnichsen, F. D.; Tuzek, F.; Herges, R. Magnetic Bistability of Molecules in Homogeneous Solution at Room Temperature. *Science* **2011**, *331*, 445–448.
- (31) Calbo, J.; Weston, C. E.; White, A. J. P.; Rzepa, H. S.; Contreras-García, J.; Fuchter, M. J. Tuning Azoheteroarene Photoswitch Performance through Heteroaryl Design. *J. Am. Chem. Soc.* **2017**, *139*, 1261–1274.
- (32) Travieso-Puente, R.; Budzak, S.; Chen, J.; Stacko, P.; Jastrzebski, J. T. B. H.; Jacquemin, D.; Otten, E. Arylazindazole Photoswitches: Facile Synthesis and Functionalization via S_NAr Substitution. *J. Am. Chem. Soc.* **2017**, *139*, 3328–3331.
- (33) Ferreira, R.; Nilsson, J. R.; Solano, C.; Andréasson, J.; Grotli, M. Design, Synthesis and Inhibitory Activity of Photoswitchable RET Kinase Inhibitors. *Sci. Rep.* **2015**, *5*, 9769.
- (34) Stricker, L.; Fritz, E.-C.; Peterlechner, M.; Doltsinis, N. L.; Ravoo, B. J. Arylazopyrazoles as Light-Responsive Molecular Switches in Cyclodextrin-Based Supramolecular Systems. *J. Am. Chem. Soc.* **2016**, *138*, 4547–4554.

(35) Devi, S.; Saraswat, M.; Grewal, S.; Venkataramani, S. Evaluation of Substituent Effect in Z-Isomer Stability of Arylazo-1H-3,5-Dimethylpyrazoles – Interplay of Steric, Electronic Effects and Hydrogen Bonding. *J. Org. Chem.* **2018**, *83*, 4307–4322.

(36) Dalko, P. I.; Moisan, L. In the Golden Age of Organocatalysis. *Angew. Chem., Int. Ed.* **2004**, *43*, 5138–5175.

(37) *N-Heterocyclic Carbenes in Transition Metal Catalysis*; Glorius, F., Ed.; Topics in Organometallic Chemistry; Springer: Berlin, 2007.

(38) Evenson, S. J.; Mumm, M. J.; Pokhodnya, K. I.; Rasmussen, S. C. Highly Fluorescent Dithieno[3,2-*b*:2',3'-*d*]Pyrrole-Based Materials: Synthesis, Characterization, and OLED Device Applications. *Macromolecules* **2011**, *44*, 835–841.

(39) Joule, J. A. Natural Products Containing Nitrogen Heterocycles—Some Highlights 1990–2015. In *Adv. Heterocycl. Chem.*; Academic Press, New York, 2016; Vol. 119, pp 81–106.

(40) Vitaku, E.; Smith, D. T.; Njardarson, J. T. Analysis of the Structural Diversity, Substitution Patterns, and Frequency of Nitrogen Heterocycles among U.S. FDA Approved Pharmaceuticals: Mini-perspective. *J. Med. Chem.* **2014**, *57*, 10257–10274.

(41) Otsuki, J.; Suwa, K.; Narutaki, K.; Sinha, C.; Yoshikawa, I.; Araki, K. Photochromism of 2-(Phenylazo)Imidazoles. *J. Phys. Chem. A* **2005**, *109*, 8064–8069.

(42) Weston, C. E.; Richardson, R. D.; Haycock, P. R.; White, A. J. P.; Fuchter, M. J. Arylazopyrazoles: Azoheteroarene Photoswitches Offering Quantitative Isomerization and Long Thermal Half-Lives. *J. Am. Chem. Soc.* **2014**, *136*, 11878–11881.

(43) Kolarski, D.; Szymanski, W.; Feringa, B. L. Two-Step, One-Pot Synthesis of Visible-Light-Responsive 6-Azopurines. *Org. Lett.* **2017**, *19*, 5090–5093.

(44) Liang, F.; Li, S.; Lindsay, S.; Zhang, P. Synthesis, Physicochemical Properties, and Hydrogen Bonding of 4(5)-Substituted 1-H-Imidazole-2-Carboxamide, a Potential Universal Reader for DNA Sequencing by Recognition Tunneling. *Chem. - Eur. J.* **2012**, *18*, 5998–6007.

(45) Kamlet, M. J.; Abboud, J. L.; Taft, R. W. The Solvatochromic Comparison Method. 6. The.Pi.* Scale of Solvent Polarities. *J. Am. Chem. Soc.* **1977**, *99*, 6027–6038.

(46) Wendler, T.; Schütt, C.; Näther, C.; Herges, R. Photo-switchable Azoheterocycles via Coupling of Lithiated Imidazoles with Benzenediazonium Salts. *J. Org. Chem.* **2012**, *77*, 3284–3287.

(47) Xu, Y.; Gao, C.; Andréasson, J.; Gröthli, M. Synthesis and Photophysical Characterization of Azoheteroarenes. *Org. Lett.* **2018**, *20*, 4875–4879.

(48) Alabugin, I. V. *Stereoelectronic Effects: A Bridge between Structure and Reactivity*; Wiley: Chichester, West Sussex, U.K.; Hoboken, NJ, 2016.

(49) Glendening, E. D.; Badenhop, J. K.; Weinhold, F. Natural Resonance Theory: III. Chemical Applications. *J. Comput. Chem.* **1998**, *19*, 628–646.

(50) Weinhold, F.; Landis, C. R. *Discovering Chemistry with Natural Bond Orbitals: Weinhold/Discovering Chemistry*; John Wiley & Sons, Inc.: Hoboken, NJ, 2012.

(51) Glendening, E. D.; Landis, C. R.; Weinhold, F. NBO 6.0: Natural Bond Orbital Analysis Program. *J. Comput. Chem.* **2013**, *34*, 1429–1437.

(52) Ramsden, C. A. The Influence of Aza-Substitution on Azole Aromaticity. *Tetrahedron* **2010**, *66*, 2695–2699.

(53) Chen, J.; Yin, Z. Cooperative Intramolecular Hydrogen Bonding Induced Azo-Hydrazone Tautomerism of Azopyrrole: Crystallographic and Spectroscopic Studies. *Dyes Pigm.* **2014**, *102*, 94–99.

(54) Hasegawa, Y.; Kume, S.; Nishihara, H. Reversible Light-Induced Magnetization Change in an Azobenzene-Attached Pyridylbenzimidazole Complex of Iron(ii) at Room Temperature. *Dalton Trans* **2009**, *2*, 280–284.

(55) Dolles, D.; Strasser, A.; Wittmann, H.-J.; Marinelli, O.; Nabissi, M.; Pertwee, R. G.; Decker, M. The First Photochromic Affinity Switch for the Human Cannabinoid Receptor 2. *Adv. Ther.* **2018**, *1*, 1700032.